



Kinematics of the broad absorption line region in QSOs: Rotation and random motion

E. Lyratzi^{a,b,*}, L.Č. Popović^c, E. Danezis^a, M.S. Dimitrijević^{c,d}, A. Antoniou^a

^a University of Athens, Faculty of Physics, Department of Astrophysics, Astronomy and Mechanics, Panepistimioupoli, Zographou 157 84, Athens, Greece

^b Eugenides Foundation, Syngrou 387, 175 64 P. Faliro, Greece

^c Astronomical Observatory, Volgina 7, 11060 Belgrade, Serbia

^d Observatoire de Paris, LERMA CNRS UMR 8112, 5 Place Jules Janssen, 92190 Meudon, France

ARTICLE INFO

Article history:

Available online 8 October 2009

PACS:

98.62.Ra

Keywords:

Active galactic nuclei

Broad line regions

Broad absorption line regions

ABSTRACT

Assuming that the Broad Absorption Line Region – BALR (originated in a disk wind) is composed of a number of successive independent absorbing density layers, which have apparent rotational and radial velocities and where ions have random velocities, we applied a model in order to obtain the kinematical parameters of BALR, by fitting the broad absorption lines. The model can be easily used in fitting the observed absorption lines, providing us with basic kinematical parameters of BALR (random, rotational and radial velocities). Fitting broad absorption lines of several BALQSOs observed with the HST we discuss the fraction of the rotation and random motion in the BALR. Moreover, using the obtained parameters from the best fit we discuss the general characteristics of the BALR which are in support of the disk wind origin of the region.

© 2009 Elsevier B.V. All rights reserved.

1. Introduction

Approximately about 10% of all quasars are with broad, blue-shifted absorption lines. The outflow velocity can reach up to 0.1–0.2 *c*. Usually, in their spectra the high ionization species as C IV λ 1549, Si IV λ 1397, N V λ 1240 and Ly α lines have been observed. Rarely some low ionization lines, such as Mg II λ 2798 and Al III λ 1857, also exhibit broad absorption lines (see e.g. Hamann et al., 1993; Crenshaw et al., 2003). Broad absorption lines can have different shapes. Also different types of these objects may have differences in their continua (Reichard et al., 2003).

A fundamental issue in the study of the BALR is to determine their geometry and origin. No compelling evidence in favor of a specific picture exists, and the uncertainty in these issues is hampering our attempts to obtain a complete physical model for the flows. One of the wide accepted models is that of a disk wind creating the BALR (see e.g. de Kool and Begelman, 1995; Murray and Chiang, 1995; Proga, 2003; Proga and Kallman, 2004). The natural origin of the ejected material is a disk wind that can explain the

prevalence of detached and multi absorption components seen in the BALRs. The disk wind model for BALQSOs has been proposed (see Murray and Chiang, 1998; Elvis, 2000; Proga et al., 2000; Proga, 2003; Proga and Kallman, 2004 and references therein), considering that a wind from an accretion disk is shielded from highly ionized gas ($U \sim 10$) which has a high column density ($\sim 10^{23} \text{ cm}^{-2}$) in soft X-rays.

The spectrum of a Broad Absorption Line Quasar (BALQSO) is usually interpreted as a combination of (i) a broadband continuum arising from the central engine, (ii) the broad emission lines coming from the Broad Emission Line Region (BELR), emerging near the center of the QSO and (iii) the broad absorption lines that are superposed, originating in a separate outlying region – Broad Absorption Line Region (BALR). But, it is also possible, that line emission and absorption occur in the same line-forming region (Branch et al., 2002). An important question is: Which are the physical connections between the BLR and BALR? This is also important, since at least a part of the BLR seems to be originated from wind of accretion disk (see Murray and Chiang, 1998; Popović et al., 2004). Additionally, one question is: Where is placed the BALR with respect to the center of a BALQSO and the Broad Line Region? To answer this question, one should investigate the kinematical properties of the emission and absorption lines.

The aim of this paper is to investigate kinematical properties of the BALR using a relatively simple model (see Danezis et al., 2007, this issue) that is able to calculate all expected velocities of the absorbing gas and may indicate the location of the BALR. In Sec-

* Corresponding author. Address: University of Athens, Faculty of Physics, Department of Astrophysics, Astronomy and Mechanics, Panepistimioupoli, Zographou 157 84, Athens, Greece. Tel.: +30 210 7276792.

E-mail addresses: elyratzi@phys.uoa.gr (E. Lyratzi), lpopovic@aob.bg.ac.yu (L.Č. Popović), edanezis@phys.uoa.gr (E. Danezis), mdimitrijevic@aob.bg.ac.yu (M.S. Dimitrijević), ananton@phys.uoa.gr (A. Antoniou).

tion 2 we shortly present the model, in Section 3 we apply the model to the UV spectral lines of several BALQSOs observed with the HST and discuss obtained results and finally in Section 4 the conclusions are given.

2. Theoretical models of BALR

The scattering of resonance-line photons can provide the radiative acceleration that at least partially drives BAL outflows (Arav et al., 2001). The difficulty arises in accelerating the gas to quite large velocities without completely stripping the resonance-line absorbing ions of their electrons. The disk wind model of Murray and Chiang (1998) and references therein has been very successful in explaining this and other properties of BAL quasars. In this model, a wind from an accretion disk is shielded from soft X-rays by a high column density ($N_H \sim 10^{23} \text{ cm}^{-2}$) of highly ionized gas ($U \approx 10$).

The quasar structure proposed by Elvis (2000) also assumed a disk wind, but from a narrow range of radii, such that BAL quasars are only observed when the line-of-sight is directly aligned with the wind (Crenshaw et al., 2003). A recent summary of theoretical and computational modeling of disk winds can be found in Proga et al. (2000). Some BAL quasars, particularly LoBALs, may be quasars cocooned by dust and gas rather than quasars with disk winds (Becker et al., 2000), but the only serious modeling relevant to this alternative has been the work of Williams et al. (1999).

It is clear that BAL quasars remain an active area of research. Disk wind models explain many properties of BAL quasars, but it is unclear if they can explain the full range of BAL trough profiles and column densities.

2.1. GR model – Stellar vs. quasar complex absorption lines

Hot stars with emission lines (Oe and Be) show similar phenomena in their spectra (see Fig. 1). Beside the P-Cyg profile that indicates stellar wind, there are also the so called Discrete Absorption Components – DACs (Bates and Halliwell, 1986) or Satellite Absorption Components – SACs (see Danezis et al. (2003) and Danezis et al. (2007, this issue)). These components indicate some combination of stellar wind with (apparent) spherical density regions that may lie in the disc around the stars. These density regions may have the form of shells, blobs or puffs. As a result in spectra of Oe and Be stars a number of lines, also detected in spectra of BALQSO, have very complex line profiles. In some cases the line shapes of quasars and hot emission stars are very similar (see e.g. Danezis et al., 2006). As one can see in Fig. 1, the C IV UV doublet of PG 0946+301 (up) and star HD 45910 (down) show similar phenomena, i.e. in both objects there is a blue-shifted component that indicates ejection of matter. It seems that the absorbing regions in hot emission stars and quasar present very similar spectroscopic phenomena, but with different velocity scales, i.e. in the case of a star the velocity of the wind is around several hundreds kilometers/seconds, but in the case of a quasar it is one order magnitude higher. This motivated us to apply a model developed to investigate kinematics of regions creating DACs and SACs in hot stars (in more details see Danezis et al., 2007) to BAL of quasars in order to study the kinematical parameters of BALR.

Based on this idea, we assumed that the BALR and BELR are composed of a number of successive independent absorbing/emitting density layers of matter (that are originated in a disk wind), which have apparent rotational and radial velocities and where ions have random velocities.

Here we will start from the point that absorbing region has three apparent velocities (projected on the line-of-sight of an ob-

server); (i) velocity of outflow, (ii) random velocity in the BALR and (iii) possible rotational velocity, since BALR should be affected by super-massive black hole.

Note here that random motion can be related to the motion of ions, but also, as it is often considered in the case of BELR, it can be related to clouds of gas moving in orbits with different inclinations and eccentricities. In principle, in BELR it can be considered, since we expect that the BELR is composed from a number of emitting clouds, but in the case of BALR, we expect that we have ejected stream of matter that absorbs in a line (which is shifted to the blue) and this effect of randomly distributed clouds should be significantly smaller than in the case of BELR. But such effects probably exist, at least as the differential rotational velocity projected to the line-of-sight of a stream of ejected matter. Since we extract the kinematical parameters from line profile, taking into account this effect, we are able only to give estimates for rotation and random velocities (i.e. maximal and minimal values of the velocities).

2.2. BAL profile simulations using the model

Using the GR model (Lyrtzi and Danezis, 2004; Danezis et al., 2007, this issue), first we simulate different line profiles. As one can see in Figs. 2 and 3, the model can very well reproduce the complex line shapes observed in BALQSOs. As it was mentioned above, the aim of the paper is to investigate contribution of the rotational component to broad absorption lines and location of this region with respect to the BELR. In order to simulate different position of the BALR and BELR, using the model, we simulated four cases taking (see Fig. 2):

- (a) The BELR is covered by BALR and the random velocity in the BALR is dominant ($V_{rand}/V_{rot} = 10$, Fig. 2a).
- (b) The BALR is covered by BELR and the random velocity is the same as in the case (a), see Fig. 2b.
- (c) The BELR is covered by BALR and the rotational velocity in the BALR is dominant, see Fig. 2c.
- (d) The BALR is covered by BELR and the rotational velocity in the BALR is dominant, see Fig. 2d.

In Fig. 2, we simulated a composed line profile, where we assume that we have one emitting region (with only random motion FWHM = 2000 km/s) and two absorbing regions with $V_{rad1} = -2000 \text{ km/s}$ and $V_{rad2} = -1000 \text{ km/s}$, and different values of $V_{rand} = 2000 \text{ km/s}$ and $V_{rot} = 200 \text{ km/s}$ (Fig. 2a and b) and $V_{rand} = 200 \text{ km/s}$ and $V_{rot} = 2000 \text{ km/s}$ (Fig. 3a and b). Also we assume that BELR is covered by BALR (Fig. 2a and c) and vice versa (Fig. 2b and d).

As one can see from Fig. 2, even if one uses the same kinematical parameters for the BALR and BELR, the profiles can be significantly different for different cases mentioned above. But we can note some similarities, e.g. in the case where BALR is covered by BELR, the emission component of the line is more intensive (in both cases where V_{rot} or V_{rand} is dominant) than in the case when BELR is covered by BALR.

On the other hand, in the case where random motion is dominant ($V_{rand}/V_{rot} = 10$), the whole absorption profile is more symmetric than in the case where the rotation is dominant. Comparing by eye the line shapes obtained from model with ones registered in the spectra of BALQSOs one can conclude that all of the mentioned cases may be present.

We note here, that the proposed model is relatively simple, aiming to describe the regions where the spectral lines are originated. The model allow us to assume dominant rotation or random motion, and find which of them is predominant. Also, we are able

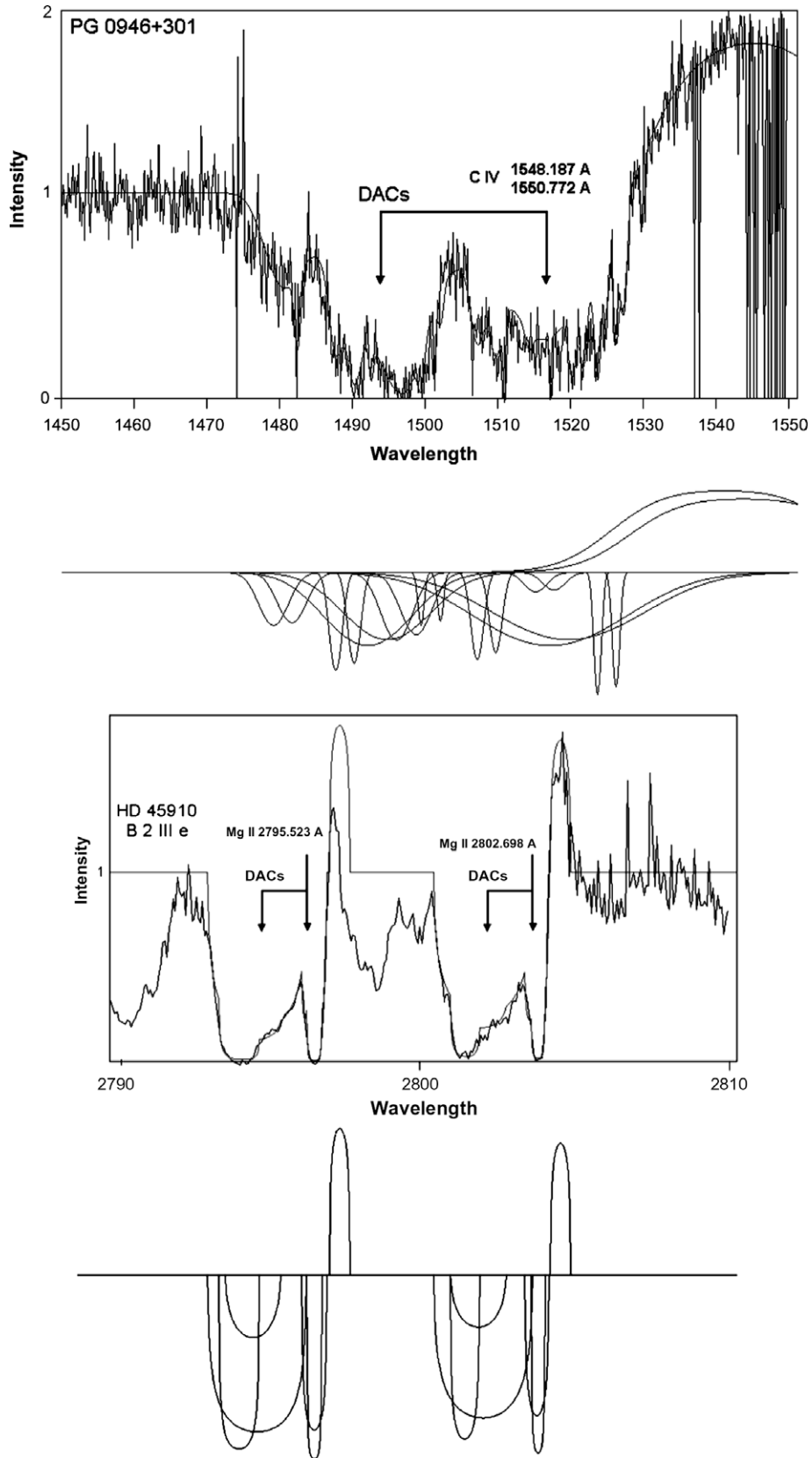


Fig. 1. The C IV UV doublet line profiles of quasar PG 0946+301 (up) and HD 45910 star (down).

to discuss the relationship between emission and absorption components for a line, considering possible connection between broad

emission and absorption line regions in sense of which of them is closer to the central black hole.

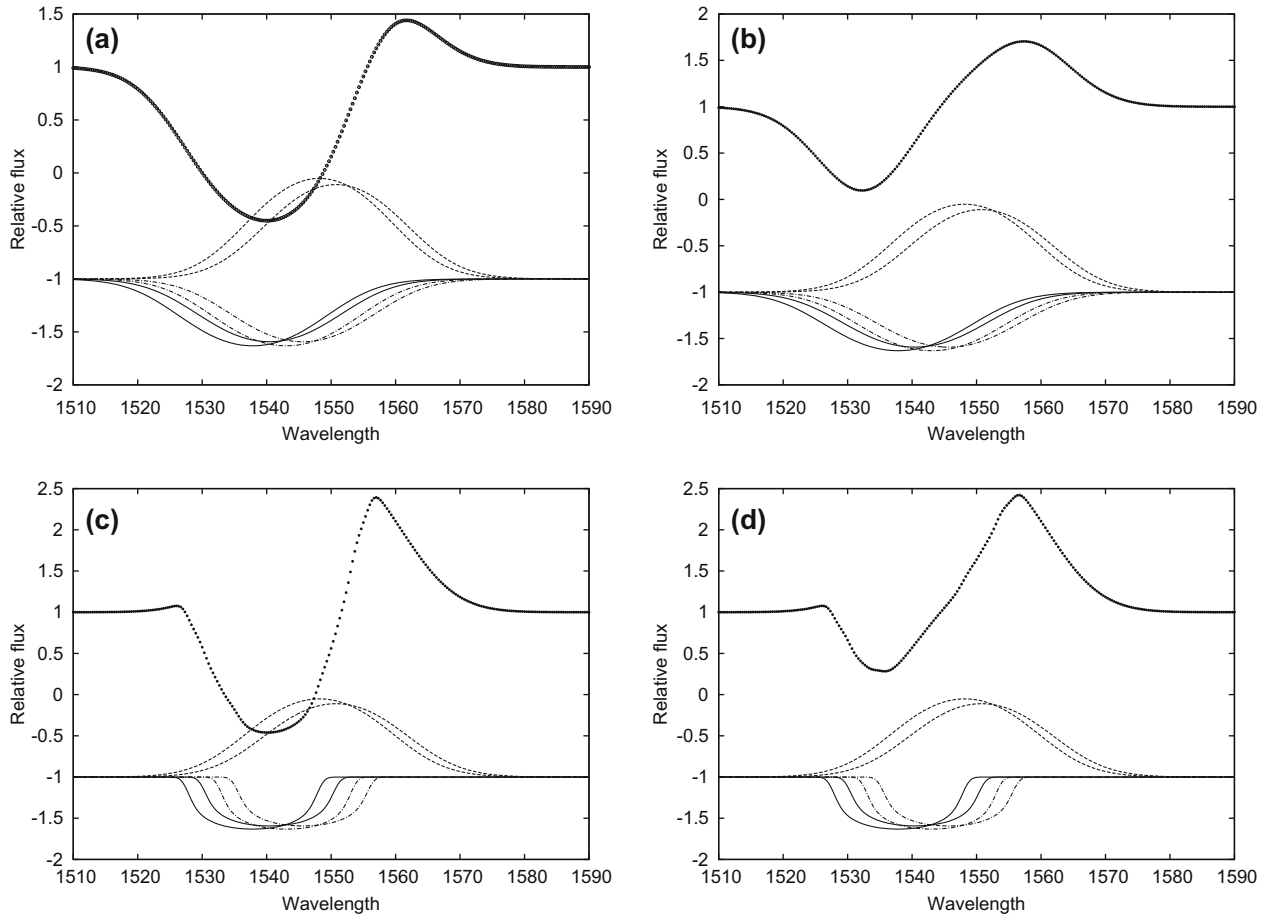


Fig. 2. The modeled CIV doublet, where an emission ($V_{rad} = 0$ km/s) and two absorption regions ($V_{rad1} = -1000$ km/s, $V_{rad2} = -2000$ km/s) were assumed: (a) dominant random velocity ($V_{rand} = 2000$ km/s, $V_{rot} = 200$ km/s for both absorption regions) and assumption that emission region is located before absorption one; (b) the same as (a) but assumption that absorption region is located before emission; (c) the same as (a) the rotational component is dominant ($V_{rot} = 2000$ km/s, $V_{rand} = 200$ km/s for both absorption regions); (d) the same as (b) but the rotational component is dominant and has value as in (c). The composed profile is present with dots and components of the profile are shown below.

3. Model application

3.1. Observations and fitting procedure

We apply the model described above to the spectra of several BALQSOs observed with the HST given in Table 1. In the Table 1, the name of the QSOs, the dates of observations and Instrument/gratings are given, as well as the lines which were fitted. The obtained spectra have resolution from 1.2 and 3.2 Å which is relatively good for application of the model. In order to scale to rest wavelength we use DIPSO software to elaborate the spectra.

A problem is that in the case of BALR, one can expect contribution of the random motion, and the line shapes are complex (i.e. rotation can be hidden by some additional narrow components which are frequently registered in the spectra of BALQSOs). To avoid this problem, we fitted the observed line using two approaches when we start with fit; (a) taking that random velocity is maximal and rotational component is minimal (in this case we will say that it is GR approach), (b) taking that rotational component is dominant (so called RG approach). After that we used F -test to conclude which approach of the model is more appropriate to explain the complex absorption lines.

As it is well known the relevant broadening mechanisms in the case of BAL is random motion of absorbing gas, but also, a part of rotation caused by massive black hole can be present. To find limits for rotational and random velocities, we fitted the lines assuming

first that random motion is dominant (here we call it GR model) and second that rotation is dominant (RG model).

3.2. Results from the best fit

Here, we are looking for the rotational component only in the broad absorption lines, while the narrow components were fitted assuming that there is not rotational component. This assumption was checked for several lines and it was clear that the rotational component in the narrow lines is not present. In Fig. 3 we present as an example, the fits for H 1413+1143 and PG 1700+518. As one can see from Fig. 3 the model is able to fit lines assuming one or more absorbing components. Here we fitted the broad Ly α and C IV components of BALQSOs listed in Table 1.

The results of the best fit are presented in Table 2. In Table 2, the estimations (minimal and maximal value respectively) for random and rotational velocities as well as radial (outflow) velocity are given. It is clear that in both cases, where we applied RG or GR approach, the outflow velocity remains the same.

As one can see from Table 2, the rotational velocity in the BALR has lower limit of ~ 100 km/s, that is corresponding to the low rotation (as e.g. the stars in the galactic disc). But in the case of the broad absorption lines (with large FWHM), the maximal value of the rotation reaches the value of several 1000 km/s. We found that the maximal value corresponds to the case of the C IV line of PG 1700+518, where a maximal rotation of 6500 km/s may be present. As one can

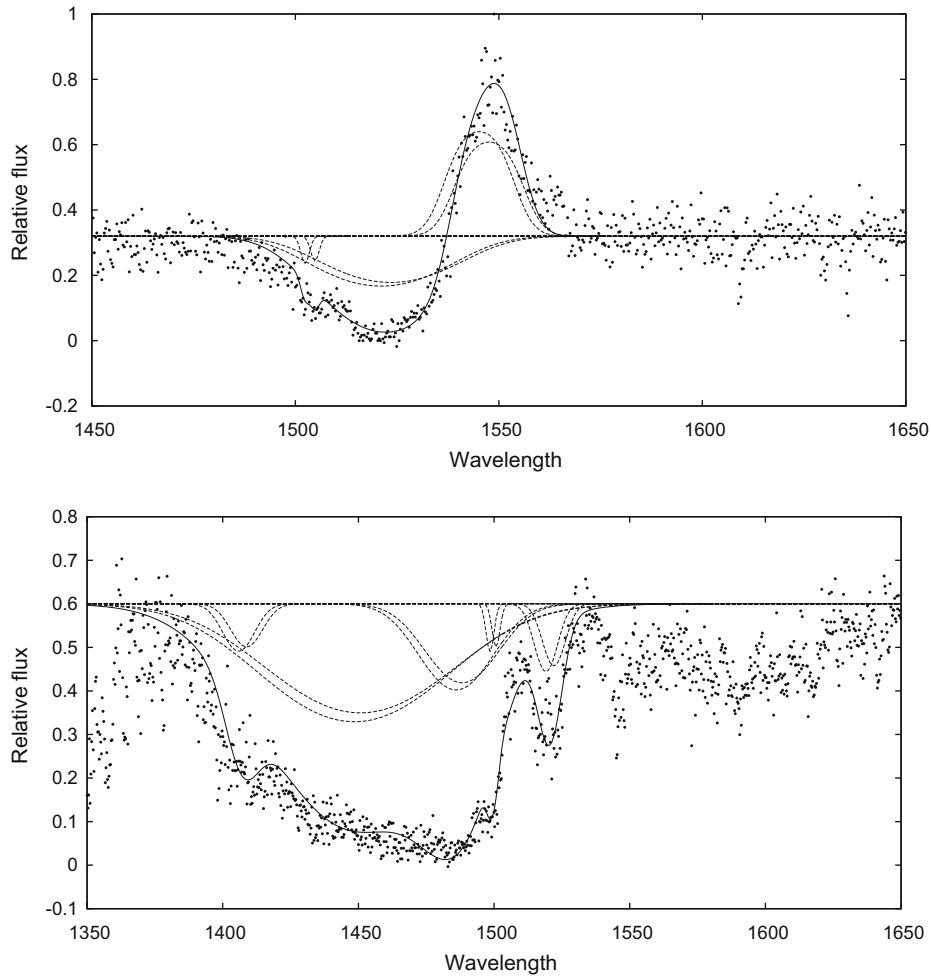


Fig. 3. The C IV line (dots) fitted with the model (solid line) for H1413+1143 and PG 1700+518 quasar. The components of the best fit are shown below.

Table 1

The list of selected BAL QSOs with basic observational data.

Name	Z	Class	Obs. date	Ins./grat.	Lines
PG 0946+301	1.216	BAL QSO	February 16, 1992	FOS/G400,G570	Ly, Si IV, C IV
PG 1700+518	0.292	BAL QSO	September 12, 2000	STIS/G430L,G750L	Si IV, C IV
UM 425	1.462	BAL QSO	November 8, 1994	FOS/G270H	O VI, Ly
HS 1216+5032B	1.45	BAL QSO	June 11,1996	FOS/G270H	Ly
H 1413+1143	2.551	BAL QSO	June 23, 1993, December 23, 1994	FOS/G400H,G570H	Ly, Si IV, C IV
PG1254+047	1.024	BAL QSO	February 17,1993	FOS/G160L,G270H	OV, O VI, Ly, Si IV, C IV
QSO 0957+561	1.41	BAL QSO	October 20,1995	FOS/G270H	Ly

see in Fig. 4, the C IV lines of this BALQSO have no emission component. Also, it is interesting, that maximal value of the rotational velocity decreases when the emission is present in the line.

Additionally, one can speculate that the rotation measured in lines, is caused by gravitational field of massive black hole in the center of BALQSOs than one can estimate distance of BALR using a simple relation $R[R_g] \approx (c/V_{rot})^2$, where R is given in gravitational radii ($R_g = GM_{bh}/c^2$, where G is the gravitational constant, M_{bh} is the mass of central black hole and c is the velocity of light).

As e.g. in the case of PG 1700+518, the C IV absorbing region can be located at $\sim 2000R_g$ that may be closer than the place of the Broad Emission Line Region. It can explain why the emission in PG 1700+518 C IV lines is not present.

On the other hand, taking an average value of the rotational velocity only of broad absorption lines and calculating the location of the BALR using the rotational velocity, we can conclude that it is

located around several times of $10^4 R_g$. The distance is not so far from the central massive black hole and it should be considered that the model of resonance scattering, where the UV line emission and absorption occur in the same line-forming region (Branch et al., 2002), is relevant to explain BALR.

It is interesting to see some connection between kinematical parameters obtained from the best fit. We discuss, so called averaged random and rotational velocities obtained as $\langle V \rangle = (V_{max} + V_{min})/2$. In Fig. 5 we plot the $|V_r/FWHM|$ against the averaged rotation (crosses) and random (squares) velocities. As one can see in Fig. 5, for smaller $|V_r/FWHM|$, the differences between averaged rotational and random velocity are larger. On the other hand, when $|V_r/FWHM| > 5$, there are small averaged random and rotational velocities and the difference between them is small. For $|V_r/FWHM| < 5$ the random velocity is dominant and has a trend to increase as the $|V_r/FWHM|$ decreases. This can be expected, as, in

Table 2
The parameters of broad absorption line components. The limits for the random and rotational components in the BAL (V_{rand}^{min} , V_{rand}^{max} , V_{rot}^{min} , V_{rot}^{max}) are given. Assuming that rotational component coming from the gravitation of the central black hole, the limits for the place of origin of the BAL is given.

Object	Line	V_{rand}^{min} (km/s)	V_{rand}^{max} (km/s)	V_{rad} (km/s)	FWHM (km/s)	V_{rot}^{min} (km/s)	V_{rot}^{max} (km/s)
PG0946+301	Ly α	960	1480	-5060	3882	500	1800
		1120	1450	-12,947	3119	100	1000
	C IV	615	2143	-5998	4672	600	3000
		615	1208	-10,833	2704	600	1800
		230	456	-10,061	982	100	600
PG1700+518	C IV	2	342	-6385	706	100	700
		5700	6953	-19,348	15,352	150	6500
		2280	2850	-12,092	6094	100	3000
		1140	1277	-27,474	2650	200	1000
		456	912	-5611	1924	125	1000
UM425	Ly α	114	319	-9674	671	100	800
		291	872	-8804	1826	100	1000
HS1216+5032B	Ly α	116	291	-17,953	801	300	500
H1413+1143	Ly α	440	784	-5919	2282	100	1200
		580	1162	-8557	2708	100	1200
PG1254+047	C IV	2280	3191	-5224	7103	100	3600
		1600	1860	-14,303	4720	100	1500
QSO0957+561	Ly α	1600	1976	-19,235	4811	100	1500
		1595	1938	-5804	3977	100	1000
QSO0957+561	Ly α	350	581	-2219	1740	100	700

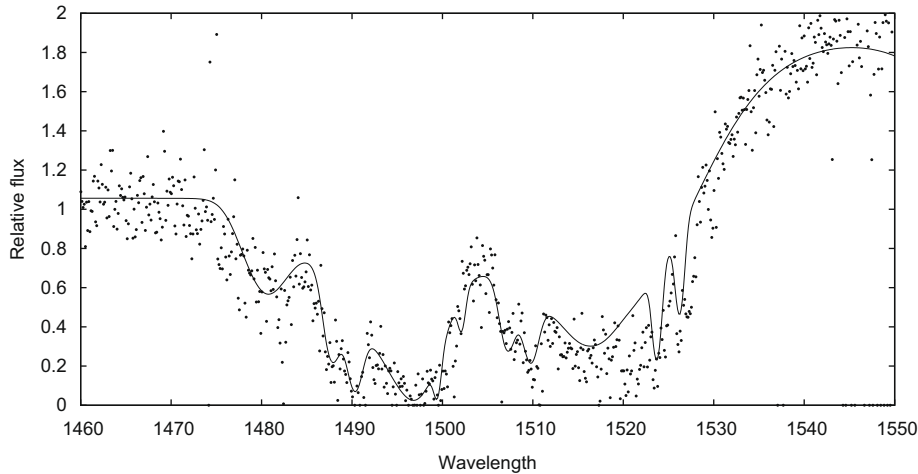


Fig. 4. The C IV line (dots) fitted with the model (solid line) for PG 0946+30 quasar.

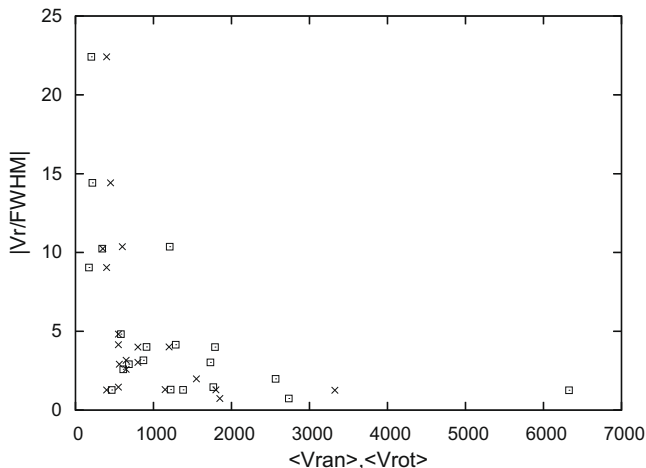


Fig. 5. Normalized radial velocity to FWHM ($|V_r|/FWHM$) against the averaged rotation (crosses) and random (squares) velocities.

the case of small outflow velocity, the wind of some AGNs may have the form of clouds or blobs. In that case the random velocity is more dominant.

4. Conclusion

Assuming that BALR is composed of a number of successive independent absorbing density layers, which have constant rotational and radial velocity we applied the model, developed to explain hot emission stars' spectra by Danezis et al. (2007, this issue), to BAL and we can outline that:

1. The model can simulate BALs taking into account a high velocity outflow.
2. The model can well fit the observed broad absorption line profiles (absorption as well as emission) and give us estimates of the random, rotational and radial velocities in the BALR.

To estimate kinematical parameters of BALR we fitted BALs, Ly α and C IV, of several BALQSOs (see Table 1) and found that:

1. The BALR is very often composed of several subregions which have different kinematical parameters, where all three kinematical component can be detected (see Table 2).
2. There is indication of a rotation component, that is at least of the order of several hundreds kilometers. If one speculates that it is connected with rotation of absorbing gas around super-massive black hole, the position of BALR is \sim several $10^4 R_g$, what is comparable with the position of the BLR.
3. In some objects, as e.g. in PG 1700+518 and PG 0946+30, a strong absorption (without emission) component indicates higher rotational velocities and consequently closer BALR than BLR to super-massive black hole.

Finally, we can conclude that the BALs seem to be produced at the same place (or even closer) as BELs and that this result is in the favor of the models that assume the forming line region as the region which emits broad emission and absorption lines, as e.g. resonance scattering model (Branch et al., 2002).

Acknowledgments

This research project is progressing at the University of Athens, Department of Astrophysics, Astronomy and Mechanics, under the financial support of the Special Account for Research Grants, which we thank very much. This work also was supported by Ministry of Science of Serbia, through the projects “Influence of collisional pro-

cesses on astrophysical plasma line shapes” and “Astrophysical spectroscopy of extragalactic objects”.

References

- Arav, N., De Kool, M., Korista, K.T., et al., 2001. *ApJ* 561, 118.
 Bates, B., Halliwell, D.R., 1986. *MNRAS* 223, 673.
 Becker, R.H., White, R.L., Gregg, M.D., Brotherton, M.S., Laurent-Muehleisen, S.A., Arav, N., 2000. *ApJ* 538, 72.
 Branch, D., Leighly, K.M., Thomas, R.C., Baron, E., 2002. *ApJL* 578, L37.
 Crenshaw, M.D., Kraemer, S.B., George, I.M., 2003. *ARAA* 41, 117.
 Danezis, E., Nikolaidis, D., Lyratzi, V., Stathopoulou, M., Theodosiou, E., Kosionidis, A., Drakopoulos, C., Christou, G., Koutsouris, P., 2003. *AP&SS* 284, 1119.
 Danezis, E., Popović, L.Č., Lyratzi, E., Dimitrijević, M.S., 2006. *AIP Conf. Proc.* 876, 373.
 Danezis, E., Nikolaidis, D., Lyratzi, E., Popović, L.Č., Dimitrijević, M.S., Antoniou, A., Theodosiou, E., 2007. *PASJ* 59, 827.
 Danezis, E., Lyratzi, E., Popović, L.Č., Dimitrijević, M.S., Antoniou, A., this issue, *NewAR*.
 de Kool, M., Begelman, M.C., 1995. *ApJ* 455, 448.
 Elvis, M., 2000. *ApJ* 545, 63.
 Hamann, F., Korista, K.T., Morris, S.L., 1993. *ApJ* 415, 541.
 Lyratzi, E., Danezis, E., 2004. *AIP Conf. Proc.* 740, 458–473.
 Murray, N., Chiang, J., 1995. *ApJ* 451, 498.
 Murray, N., Chiang, J., 1998. *ApJ* 494, 125.
 Popović, L.Č., Mediavilla, E., Bon, E., Ilić, D., 2004. *A&A* 423, 909.
 Proga, D., 2003. *ApJ* 592, 9.
 Proga, D., Kallman, T.R., 2004. *ApJ* 616, 688.
 Proga, D., Stone, J.M., Kallman, T.R., 2000. *ApJ* 543, 686.
 Reichard, T.A., Richards, G.T., Hall, P.B., Schneider, D.P., Vanden Berk, D.E., Fan, X., York, Donald G., Knapp, G.R., Brinkmann, J., 2003. *AJ* 126, 2594.
 Williams, R.J.R., Baker, A.C., Perry, J.J., 1999. *MNRAS* 310, 913.